

## Size effect study on compressive strength of SCLC

Mohammad Karamloo<sup>\*1</sup>, Mohammad Amin Roudak<sup>2</sup> and Hamed Hosseinpour<sup>1</sup>

<sup>1</sup>Department of Civil Engineering, Shahid Rajaei Teacher Training University, Lavizan, Tehran, Iran

<sup>2</sup>School of Civil Engineering, Iran University of Science and Technology, Narmak, Tehran 16846, Iran

(Received May 5, 2018, Revised April 13, 2019, Accepted April 23, 2019)

**Abstract.** In the present study, effect of size and placement of cubic specimens on compressive strength of self-compacting lightweight concrete (SCLC) were considered. To do so, 81 specimens of different sizes (50 mm, 75 mm, 100 mm, and 150 mm) were prepared by using three different mixes of SCLC. Results of the cured specimens were then used in regression analyses to find predictive equations with regard to both the placement direction and the size. Test results showed that the strength ratio in cases in which the direction of loading and placement were parallel, were higher than those specimens, whose configurations were normal between loading and placement. In addition, strength ratios in SCLC mixes were slightly higher than those are for self-compacting normal weight concrete. In order to analyze the effect of size on compressive strength the conventional size effect law as well as the modified size effect law (MSEL) were used. Besides, the convergence criterion of nonlinear regression process of size effect study has been discussed. Analyses of the results showed that the unconstrained nonlinear regression in size effect study of SCLC mixes could lead to erroneous results.

**Keywords:** self-compacting lightweight concrete; compressive strength; size effect; loading direction

### 1. Introduction

Concrete and cement paste possess defects, pores, and cracks with broad range of length-scales, from nanometers to millimeters (Zhang *et al.* 2018). These features make these materials complex to understand. Therefore, cementitious composites, in general, could exhibit different behavior under loading, depending either on the size (Zhang *et al.* 2018) or on their constituents (Karamloo and Mazloom 2018; Mazloom and Karamloo 2019). It has been long known that the fracture behavior and mechanical properties of quasi-brittle solids are size dependent (Gonnermann 1925, Leicester 1969, Bazant 1976, Bazant 1984, Mindess 1984, Hilsdorf and Brameshuber 1985, Bazant *et al.* 1986). However, there are still major debates about the asymptotic behavior of these materials. For instance, (Karamloo and Mazloom 2018) proposed an algorithm to circumvent the drawback of conventional size effect law of Bazant about considering the effect of notch length. In another study, Zhang and his co-workers, investigated the size effect phenomenon on splitting strength of hardened cement paste focusing on small scale samples (Zhang *et al.* 2018). In addition to the asymptotic behavior analysis in size effect study, constituents of the composite could play a leading role in global behavior of the specimen. In this regard, some researches have focused their attentions on the effect of mix design parameters on fracture behavior of concrete. For example Ince and Cetin (2018) investigated the effect of grading of aggregate on fracture parameters of normal concrete. Apart from normal

concrete, new generations of concrete including self-compacting concrete or self-compacting lightweight concrete have gathered a notable amount of attention, due to their specific characteristics such as high workability. Since the cast process of almost all of these generations of concrete necessitates large amounts of ultrafine particles as well as wide range of chemical admixtures, the microstructure of the mix would surely be affected. Therefore, with regard to the fact that the ultrafine particles increase the risk of autogenous and drying shrinkage, the cracking pattern would be different (Nikbin *et al.* 2014, Mazloom *et al.* 2017, Mazloom *et al.* 2018). Thus, further investigation about the size effect of new generations of concrete seems to be essential.

Self-compacting lightweight concrete (SCLC) is a new generation of concrete with specific engineering benefits (Karamloo *et al.* 2016, Karamloo *et al.* 2016, Karamloo *et al.* 2017, Mazloom *et al.* 2017). It has the ability to fill the complex formworks without any external vibration besides the segregation resistance (Topçu and Uygunoğlu 2010, Vakhshouri and Nejadi 2017). Moreover, the use of lightweight aggregate could lead to a more durable substance, due to the internal curing phenomenon (Zhutovsky and Kovler 2012, de Sensale and Goncalves 2014, Kim *et al.* 2016, Lotfy *et al.* 2016). It could be found out by reviewing the literature that the use of LWA in concrete could lead to a decrease of autogenous shrinkage (Bentz and Snyder 1999, Kohno *et al.* 1999, Zhutovsky *et al.* 2002, Akcay and Tasdemir 2009). Moreover, it absorbs  $\text{Ca}^{2+}$  and  $\text{OH}^-$  and releases of high amounts of  $\text{Si}^{4+}$  (Kong *et al.* 2014). Di Bella *et al.* (2012) conducted an experimental research on alkali-silica reactivity of four types of LWA. They reported that the concrete mixes with either expanded clay or expanded vermiculite showed no signs of alkali-

\*Corresponding author

E-mail: m.karamloo@srutu.edu; m.karamloo@sru.ac.ir

silica reaction. However, in the case of expanded perlite or glass, more experiments are needed. Bentz (2009) claimed that mixture containing 31% LWA and 69% normal sand (by volume) reduced chloride ion diffusivity by 25% or more. In addition to the mentioned characteristics regarding the use of LWA in concrete, SCLC has lower density than the normal concrete (NC) or self-compacting normal weight concrete (SCC). Therefore, the use of SCLC in construction industry could lead to a more cost efficient and Eco-friendly construction, because it reduces the member sizes and dead loads. In addition, by reducing the waste demolished as well as decreasing the thermal conductivity (Kim *et al.* 2012), it could be integrated with the demarche of green construction (Zarghami *et al.* 2017, Zarghami *et al.* 2018).

Apart from technical, environmental, and economical advantages regarding the use of SCLC, researches focusing on the behavior of this type of concrete are too limited (Shailendra Kumar and Barai 2012, Mazloom and Yoosefi 2013, Mazloom *et al.* 2015, Zhao *et al.* 2015, Mazloom and Mahboubi 2017, Vakhshouri and Nejadi 2017). In addition, the use of LWA, high amounts of superplasticiser, and admixtures, could raise some concerns among the researchers and practitioners about the mechanical behavior of SCLC. Amongst the mechanical properties in design of concrete structures, compressive strength is the most important property, which should be tested routinely during the construction (Nikbin *et al.* 2014). Different countries use different sizes of cubic or cylindrical specimens. On the other hand and in contrast to the classical mechanics of materials in which the strength of material is assumed size independent, size of concrete specimen could affect the test results. For instance, Gonnermann (1925), Neville (1966), Gyengo (1938), Blanks and McNamara (1935), were of the first researchers who conducted experiments on different geometries of NC specimens to determine the size effects on concrete compressive strength. Walsh (1972), was the other researcher who investigated the size effect phenomenon. He used 3-point notched beam specimens and showed that the linear elastic fracture mechanics (LEFM) does not hold for NC. Besides, his experiments revealed that there is a strong relation between the nominal strength of the notched beams and their sizes. This observation was discussed later on theoretical basis by Hillerborg *et al.* (1976), and Bazant and his co-workers (Bazant and Cedolin 1979, Bazant 1982, Bazant and Oh 1983, Bazant 1984, Bazant *et al.* 1986, Bazant and Pfeiffer 1987). After Bazant's pioneering work and introduction of size effect law (SEL) for geometrically similar notched beam specimens (Bazant 1984), a modified size effect law (MSEL) was introduced by Kim and Eo in which the effects of dissimilarity of notches were claimed to be considered (Kim and Eo 1990). In other words, they added a new term to the Bazant's SEL, which was proposed in Bazant (1984), and claimed that their prediction is better than Bazant's. About seven years later, Bazant and Xiang used the concepts of energy and crack band model (Bazant 1982, Bazant and Oh 1983) to explain size effect in compression fracture of concrete (Bazant and Xiang 1997). They concluded that in the large size specimens, the nominal strength of the specimen  $\sigma_N$ , shows the size effect

approaching the power law  $d^{-2/3}$ . Based on their conclusions, they attributed this difference with the LEFM characteristic power law ( $d^{-1/2}$ ) to the variation of the spacing of axial splitting micro-cracks (Bazant and Xiang 1997). The other research conducted for determination of size effect on compressive strength of concrete cylinders, is the study of Kim *et al.* (1999). Actually, they used nonlinear fracture mechanics for modification of the MSEL to include the effects of confinement and height to diameter ( $h/d$ ) ratio. Sim *et al.* (2013) investigated the effects of size and shape on compressive strength of lightweight concrete. They used the crack band model and derived a mathematical model in which the effects of aspect ratio, size, shape, and unit weight of concrete were reflected. Based on the mentioned study, the penetration of crack in LWA resulted in poor crack distribution and therefore localized crack zone with minority of micro-cracks (Sim *et al.* 2013). Impacts regarding the size and shape of high strength concrete specimens on its compressive strength were reported by Tokyay and Ozdemir (1997). They surprisingly claimed that the  $h/d$  ratio does not affect the compressive strength of high strength concrete cylinders. Yi and his co-workers (Yi *et al.* 2006) used the least-square-method to fit their experimental observations about compressive strength of NC to MSEL. Moreover, they considered influence of loading direction on compressive strength of NC. They claimed that the loading direction has no noticeable effect on compressive strength of NC. However, they reported different trend for high strength concrete. Yazici and Sezer (2007) conducted an experimental survey on effect of cylindrical specimen size on the compressive strength of NC. They tested eight series of mix compositions with water to cement ratios of 37%, 42%, 47%, 48%, 55%, 62%, 71%, and 77% (by volume). By testing 150×300 mm and 100×200 mm (diameter×height) cylindrical specimens, they claimed that suitable average conversion factor (the ratio of compressive strength of 100×200 to 150×300 cylinder) could be taken as 1.03 (Yazıcı and İnan Sezer 2007). With recent trend towards using SCC, Nikbin *et al.* (2014) considered the effects of cube size and direction of placement on compressive strength of SCC. The results of the mentioned study showed that influence of placement direction was obviously more important than size effect in SCC specimens.

Although they seem to be simple, the compressive fracture behavior of concrete and the impacts of loading direction and size of cubic samples are of the most questionable properties for design goals. In addition, as it can be seen from the above-mentioned literature review and to the authors' knowledge, the information about these properties of SCLC is lacking, if there is any. In this regard, in the present study, effect of loading direction and size of cubic specimens on compressive strength of the SCLC samples have been considered. Moreover, Bazant's size effect law and modified size effect law (MSEL) of Kim and Eo (1990), Bazant and Xiang (1997) were fitted to the test results.

## 2. Materials and mix proportions

Table 1 Portland cement type I-425 chemical and physical properties

Chemical Analysis	
Compounds (%)	Results
SiO <sub>2</sub>	21.05
Al <sub>2</sub> O <sub>3</sub>	4.76
Fe <sub>2</sub> O <sub>3</sub>	3.43
CaO	62.86
MgO	3.46
SO <sub>3</sub>	1.87
Na <sub>2</sub> O	0.21
K <sub>2</sub> O	0.58
CL	0.04
LOI (%)	1.2
Insoluble Residue (%)	0.53
Total	100
Composition According to BOGUE	
C <sub>3</sub> S (%)	53.4
C <sub>2</sub> S (%)	20.1
C <sub>3</sub> A (%)	6.9
C <sub>4</sub> A (%)	10.4
CaSO <sub>4</sub> (%)	3.2
CaO <sub>free</sub>	0.8
Physical Tests	
Fineness: Blaine (Cm <sup>2</sup> /g)	3307
Autoclave Expansion %	0.14
Compressive strength	
2-day (MPa)	21.48
28-day (MPa)	47.48
Setting Time (Vicat)	
Initial (min)	140
Final (hr.)	3:10

Table 2 Mixture proportioning of the used mix compositions

Mix	Contents (kg/m <sup>3</sup> )						Ratios	
	Cement (c)	Water (w)	LECA	Sand	Limestone powder (p)	Superplasticiser	w/c	w/p
W33	500	165	280	750	195	12.5	0.33	0.237
W37	500	185	280	750	195	9	0.37	0.237
W43	400	172	280	750	175	3.5	0.43	0.289

### 2.1 Material properties

In the present study, the ordinary Portland cement (CEM I 42.5N), whose physical and chemical characteristics are reflected in Table 1, was provided from Tehran cement factory. The coarse aggregate was lightweight expanded clay, which was produced by LECA. However, the fine aggregate was normal river sand whose fineness modulus was about 3. In order to enhance the workability, a polycarboxylate based superplasticiser was provided. Moreover, ultra-fine limestone powder was used for modification of the viscosity of the mix.

### 2.2 Mix compositions

In order to assess the effects regarding the size of cubic

Table 3 Fresh state properties of the SCLC mix compositions

Mix	Slump flow		U-box	V-funnel (sec)	J-ring
	Flow time (sec)	Flow diameter (mm)	Height difference (mm)		Diameter (mm)
W33	4.1	725	40	20	700
W37	4.5	675	57	24	640
W43	3.4	665	62	17.55	635

specimens and direction of loading, three different mix compositions, whose water/cement ratios (w/c) were 0.33, 0.37, and 0.43, have been prepared. The maximum nominal aggregate size ( $d_{max}$ ) in each mix was constant and equal to 12.5 mm. Table 2 reflects the designed mixes and their fresh state properties.

## 3. Experimental procedure

### 3.1 Preparation of the specimens

In order to determine the effects of specimen size and direction of loading on cubic compressive strength of SCLC, four groups of cubic specimens whose sizes were 50×50×50, 75×75×75, 100×100×100, and 150×150×150 mm<sup>3</sup>, and one group of standard cylinder (150×300 mm) were cast for each mix. To mix the compositions, the solid contents were first mixed for one minute. Afterwards, the mixture of water and superplasticiser was added to the composition and mixed for five minutes. All specimens were demoulded after 24 hours and transferred to the curing container to be cured under water 20±2°C.

### 3.2 Workability of fresh concrete

In contrary to the NC, conventional slump test is not suitable for testing the workability of SCLC. On the other hand, to the authors' knowledge, there is no standard regarding the workability of SCLC. Therefore, in the present study the EFNARC guidelines (EFNARC 2002), which is normally being used for SCC, were adopted to evaluate the fresh properties of the mix compositions. In this regard, slump flow, V-funnel, J-ring, and U-box tests have been carried out. The results are tabulated in Table 3. It is worth noting that there is no guideline or standard for assessment of fresh properties of SCLC. However, some references claimed that the margins of acceptability is wider than SCC mixes (Hubertova and Hela 2007). In the present study, although some fresh properties were beyond those recommended by EFNARC for SCC (EFNARC 2002), the mixes were cast without any external vibration. Besides, no noticeable bleeding or segregation were observed.

## 4. Results and discussion

### 4.1 Effects of loading and placement direction

Concrete is a heterogenous material, which exhibits

Table 4 Specimen dimensions and experimental results

Mix	Size (mm)	Compressive strength (MPa)							
		Parallel				Normal			
		Sample 1	Sample 2	Sample 3	Average	Sample 1	Sample 2	Sample 3	Average
W33	50×50×50	36.56	40.14	38.12	38.27	45.92	45.02	41.06	44
	75×75×75	36.16	35.96	42.5	38.21	45.62	44.06	39.89	43.19
	100×100×100	35.1	38.6	34.6	36.1	44.12	38.18	44.6	42.3
	150×150×150	37.52	33.34	34.02	34.96	37.23	39.86	45	40.7
	Standard cylinder	33.56	37.01	33.12	34.56	33.56	37.01	33.12	34.56
W37	50×50×50	27.63	31.15	29.18	29.32	44.2	36.51	35.55	38.75
	75×75×75	26.15	28.92	30.15	28.41	42.16	40.61	38.02	40.26
	100×100×100	26.4	25.6	32.6	28.2	39.6	41.15	21.55	34.1
	150×150×150	26.2	28.65	26.54	27.13	33.97	34.08	28.94	32.33
	Standard cylinder	25.01	30.06	24.43	26.5	25.01	30.06	24.43	26.5
W43	50×50×50	18.68	20.91	23.47	21.02	29.55	19.34	23.29	24.06
	75×75×75	22.11	19.12	19.56	20.26	19.12	24.13	28.15	23.8
	100×100×100	20.8	18.12	20.54	19.82	19.87	24.15	20.78	21.6
	150×150×150	18.24	19.76	18.82	18.94	23.54	19.34	20.18	21.02
	Standard cylinder	19.78	20.96	15.72	18.82	19.78	20.96	15.72	18.82

Table 5 Curve fitting results between compressive strength of standard cylinders and cubes with different sizes

Size	Placement and loading configuration	Fitting method					
		$f_{cu}=Af_c'+B$	$R^2$	$\zeta$ (origin-intercepted)	$R^2$	$\xi = m + n \log\left(\frac{f_{cu}}{q}\right)$	$R^2$
50	Parallel	$A=0.995, B=3.032$	0.874	0.907	0.863	$m=0.937, n=-0.020, q=0.503$	0.873
75	Parallel	$A=1.006, B=2.185$	0.799	0.924	0.794	$m=1.583, n=-0.338, q=0.330$	0.805
100	Parallel	$A=0.898, B=4.118$	0.760	0.958	0.739	$m=1.308, n=-0.234, q=0.843$	0.759
150	Parallel	$A=0.921, B=2.478$	0.882	0.991	0.873	$m=1.123, n=-0.09, q=0.838$	0.882
50	Normal	$A=1.113, B=5.977$	0.683	0.756	0.657	$m=1.26, n=-0.305, q=0.760$	0.676
75	Normal	$A=1.073, B=7.179$	0.661	0.754	0.622	$m=1.288, n=-0.263, q=0.315$	0.650
100	Normal	$A=1.257, B=-0.809$	0.709	0.814	0.709	$m=0.973, n=-0.645, q=19.58$	0.713
150	Normal	$A=1.136, B=1.108$	0.832	0.851	0.831	$m=0.914, n=-0.294, q=19.58$	0.834

different mechanical properties in different loading conditions and different directions. Yi *et al.* (2006) conducted a comprehensive experimental program for determination of effect of loading direction on compressive strength of NC and high strength concrete. In a same way Nikbin *et al.* (2014) considered these impacts on compressive strength of SCC. However, to the authors' knowledge, the informations about this phenomenon in SCLC is rare. In addition, existence of LWA, high amounts of powder content, and the use of superplasticisers could lead to a different behavior in comparison to other types of concrete. In this regard, specimens were tested after 28 days according to BS EN 12390-part 3 (BS EN 12390 2000). The tests were carried out in such a manner that the loading were applied in a direction parallel to the placement and normal to the direction of placement. Table 4 shows the results for compressive strength of the mixes regarding different specimen sizes. It is clear that in almost all cases when the loading direction is normal to the direction of placement, the compressive strength is higher than the cases in which the mentioned directions are parallel. This finding is in line with that reported by Nikbin *et al.* for SCC (Nikbin *et al.* 2014). The study of Yi *et al.* (2006), however,

is more controversial. They reported that the differences between compressive strength of NC in different loading directions did not show major diversity. However, the results for high strength concrete samples were in different line. In other words, based on the study of Yi *et al.* (2006), when the directions of loading and placement were parallel in NC samples, the compressive strength was smaller than the normal case. Nevertheless, the conclusion for the samples, which were made of high strength concrete, was opposing.

#### 4.2 Effects of specimen size

The relationship between the compressive strength of standard cylinders and different cubic samples for parallel directions of loading and placement are illustrated in Figs. 1-4. Three types of least square curve fitting were used to establish a correlation between the compressive strength of cubic specimens and those of cylinders. In the simplest form, the origin-intercepted linear curve fitting was used to define strength ratios by least square method (LSM) as

$$\xi = \frac{f'_c}{f_{cu}} \quad (1)$$

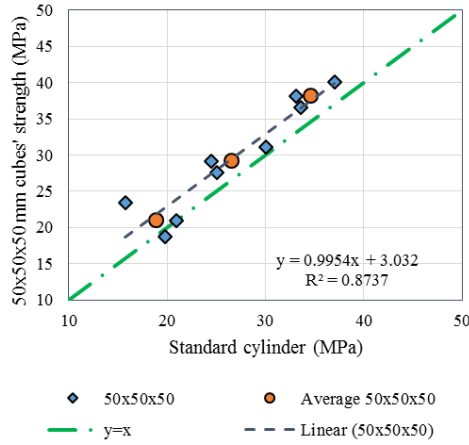


Fig. 1 Correlation between the compressive strength of 50 mm cubes and standard cylinders in parallel manner

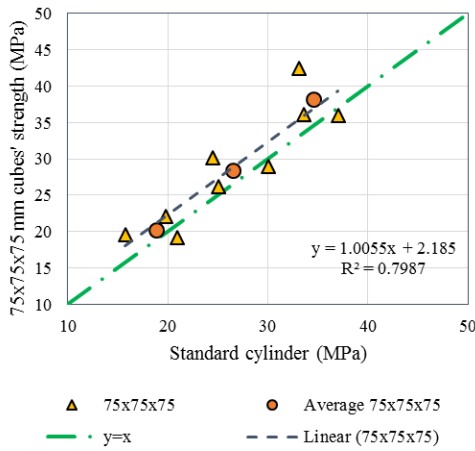


Fig. 2 Correlation between the compressive strength of 75 mm cubes and standard cylinders in parallel manner

where  $f'_c$  and  $f_{cu}$  are compressive strength of standard cylindrical specimens, and cubic samples. Table 5 shows the correlation relations between strength values of cubic specimens with those of standard cylinders. It is worth noting that  $R^2$  determines the accuracy of the results; i.e., the larger amounts of  $R^2$  shows better precisions.

As can be seen from Table 5, origin-intercepted, linear, and logarithmic types of curve fitting have been conducted for the test results. It is clear that in almost all cases,  $R^2$  values of linear form are larger than the origin-intercepted cases. Therefore, the linear form could yield better precisions. The concept of logarithmic curve fitting was borrowed from the L-Hermite's study about this phenomenon in NC (L'Hermite 1955). He stated that the relation between the strength of the standard cylinders and the  $150 \times 150 \times 150 \text{ mm}^3$  cubes is as

$$f'_c = f_{cu} \left( 0.76 + 0.2 \log \left( \frac{f_{cu}}{19.58} \right) \right) \quad (2)$$

In the present study, Levenberg-Marquardt algorithm (Moré 1978) was used to fit an equation of the form  $\xi = m + n \log \left( \frac{f_{cu}}{q} \right)$  to each series of sizes and directions.

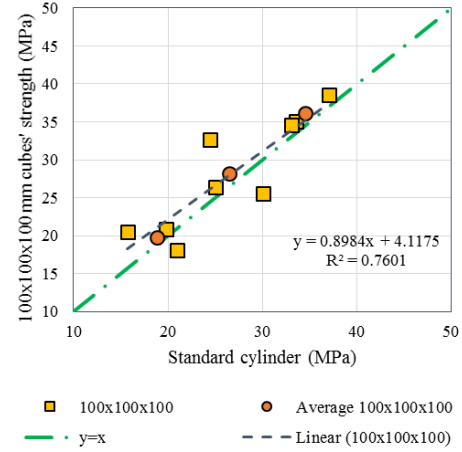


Fig. 3 Correlation between the compressive strength of 100 mm cubes and standard cylinders in parallel manner

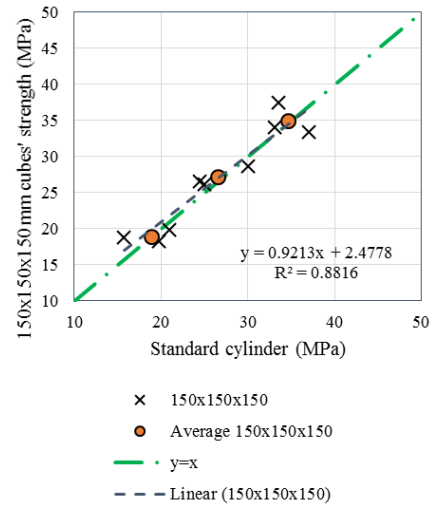


Fig. 4 Correlation between the compressive strength of 150 mm cubes and standard cylinders in parallel manner

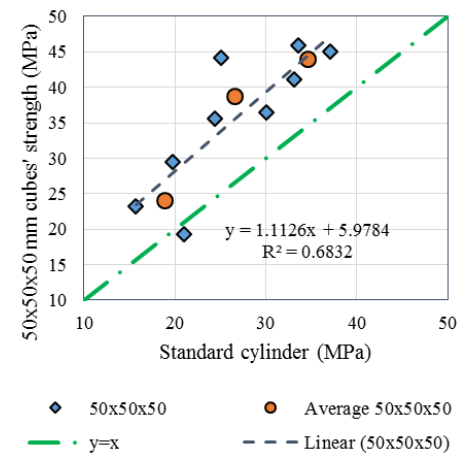


Fig. 5 Correlation between the compressive strength of 50 mm cubes and standard cylinders in normal manner

In order to compare these results with the Eq. (2) for NC and those reported for SCC (Nikbin *et al.* 2014), the value of  $q$  has been assumed to be equal to 19.58 and the results have been reflected in Table 6. It is clear in Table 5 that the

Table 6 Comparison between NC, SCC, and SCLC logarithmic forms of regression

Size	Placement and loading configuration	Type of concrete					
		SCC**		NC***		SCLC	
		$\xi = m + n \log\left(\frac{f_{cu}}{19.58}\right)$	$R^2$			$\xi = m + n \log\left(\frac{f_{cu}}{19.58}\right)$	$R^2$
50	Parallel	$m=0.70, n=0.42$	0.960	$\xi = 0.76 + 0.2 \log\left(\frac{f_{cu}}{19.58}\right)$	$m=0.905, n=-0.020$	0.873	
75	Parallel	$m=0.16, n=2.00$	0.795		$m=0.983, n=-0.338$	0.805	
100	Parallel	$m=0.42, n=1.25$	0.808		$m=0.989, n=-0.234$	0.759	
150	Parallel	$m=0.96, n=0.21$	0.944		$m=1, n=-0.09$	0.882	
50	Normal	$m=0.08, n=1.29$	0.942		$m=0.831, n=-0.305$	0.676	
75	Normal	$m=0.11, n=1.25$	0.968		$m=0.816, n=-0.263$	0.650	
100	Normal	$m=0.14, n=1.22$	0.943		$m=0.973, n=-0.645$	0.713	
150	Normal	$m=0.12, n=1.61$	0.893		$m=0.914, n=-0.294$	0.834	

\*\* See Ref (Nikbin, Dehestani *et al.* 2014) for more details;

\*\*\* See Ref (L'Hermite 1955) for more details

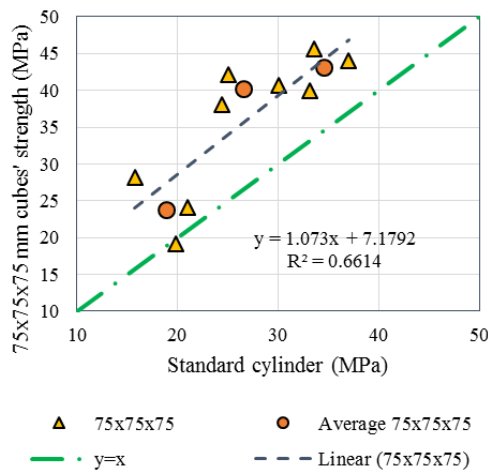


Fig. 6 Correlation between the compressive strength of 75 mm cubes and standard cylinders in normal manner

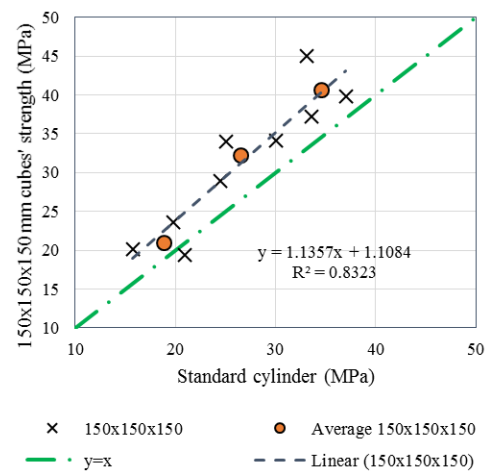


Fig. 8 Correlation between the compressive strength of 150 mm cubes and standard cylinders in normal manner

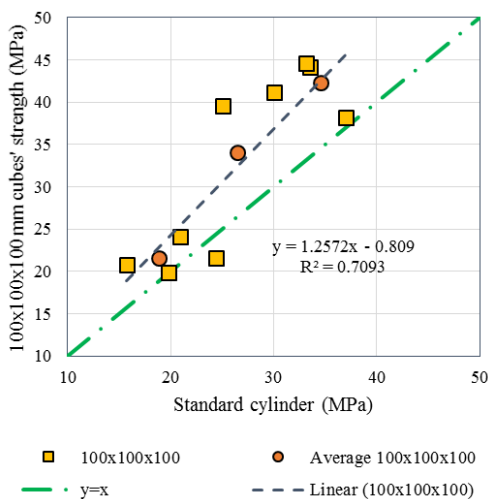


Fig. 7 Correlation between the compressive strength of 100 mm cubes and standard cylinders in normal manner

values of  $R^2$  in the logarithmic and linear forms are very close. Thus, one could use the easier linear form for sound predictions.

Figs. 5-9 shows the relationships between the compressive strength of standard cylinders and different



Fig. 9 Axial splitting cracks in a compressive test of cylindrical SCLC specimen

sizes of cubes for normal directions of loading and placement.

#### 4.3 Size effect in compressive fracture of SCLC

By testing SCLC samples, it is obvious that the compressive failure of almost all specimens under uniaxial





Fig. 10 Pattern of compressive failure in SCLC 50×50×50 and 150×150×150 mm<sup>3</sup> cubes

compression, initiates with axial splitting cracks (Fig. 9). According to Bazant's study (Bazant 1993), no release of energy occurs in these types of cracking. In other words, as stated by Bazant and Xiang (1997), since the axial splitting cracks do not change the macroscopic continuum stress state, they cannot be the mechanism of compressive failure. Nevertheless, they can trigger the macroscopic compressive failures. In this respect, Bazant and Xiang (1997) proposed that the sideways propagation of a band of parallel axial splitting cracks, in an orthogonal or inclined direction with respect to the compression direction, is the principal mechanism of compressive failure of concrete columns. It could be deduced by observing Fig. 10 that the Bazant's compressive failure theory holds for SCLC samples. The other observation that worth noting is that in contrast to the study of Nikbin *et al.* (2014), the obliqueness of failure pattern of SCLC samples were too stochastic and therefore, the authors did not observed any specific and obvious correlation between size of specimen and the obliqueness of failure pattern of SCLC cubic specimens.

The effect of size on nominal strength of specimens under tension were one of the most famous fields of study in fracture mechanics of concrete. For instance, Bazant (Bazant 1984) assumed that the width and length of fracture process zone is constant. Then, by using dimensional analysis, he described the effect of characteristic length  $d$  on nominal strength of specimen  $\sigma_N$  as

$$\sigma_N = \frac{Bf_t'}{\sqrt{1 + \frac{d}{\lambda_0 d_{\max}}}} \quad (3)$$

in which  $B$  is an empirical constant,  $f_t'$  is tensile strength,  $\lambda_0$  is an approximate constant, which is proposed to be in the range between 2.0 and 3.0 (Yi *et al.* 2006), and  $d_{\max}$  is the maximum nominal size of the coarse aggregate. The proposed  $\lambda_0$  range in the study of (Yi *et al.* 2006), however, yields unrealistic parameters. In other words, to find the values of empirical coefficients of Eq. (3), one can

manipulate this equation and propose a new coordinate system in which  $X$  axis is  $d$  and  $Y$  axis is  $\left(\frac{f_c'}{f_{cu}}\right)^2$ . By using this transformation and fitting a line  $Y=AX+C$ , the values of  $B$  and  $\lambda_0$  could be found as  $\sqrt{\frac{1}{C}}$  and  $\frac{1}{d_{\max}BA}$ , respectively. The other law is attributed to Bazant and Xiang (1997), called modified size effect law (MSEL). The MSEL is of the form

$$\sigma_N = \frac{Bf_t'}{\sqrt{1 + \frac{d}{\lambda_0 d_{\max}}}} + \alpha f_t' \quad (4)$$

where  $\alpha$  is an empirical constant. In addition, it is assumed that  $\alpha f_t'$  denotes size independent tensile strength.

In contrast to the tensile failure, the compressive failure mechanism and its size effect were not vastly investigated. However, some researchers (Yi *et al.* 2006, Nikbin *et al.* 2014), assuming that the nature of concrete compressive failure is reaching to tensile strength, used the laws mentioned in Eqs. (3) and (4) for compressive failure size effects. In the present paper, by using the proposed coordinate system, the values of  $B$  and  $\lambda_0$  could be found by simple linear regression. To illustrate this procedure, the data corresponding to the parallel configuration of mix W33, were depicted in Fig. 11. As it could be observed, the values of  $A$  and  $C$  are equal to 0.0016 and 0.7401, respectively. Hence, by using  $B = \sqrt{\frac{1}{C}}$  and  $\lambda_0 = \frac{1}{d_{\max}BA}$ ,

the values of  $B$  and  $\lambda_0$  could be found as 1.16 and 42.337 for mix W33 and parallel configuration. The results of the method for each mix and configuration are tabulated in Table 7. In addition to the proposed method, trust-region nonlinear curve fitting was used for determination of  $B$  and  $\lambda_0$ , whose results are reflected in Table 8. Moreover, for

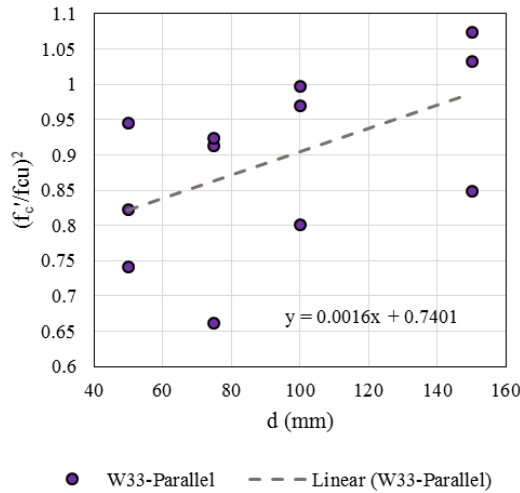


Fig. 11 Fitting a line in a proposed coordinate system for data of W33 mix in parallel configuration

Table 7 Determination of  $B$  and  $\lambda_0$  by using the proposed coordinate system

Mix ID	Placement and loading configuration	$f_{cu}(d) = \frac{Bf'_c}{\sqrt{1 + \frac{d}{\lambda_0 d_{max}}}}$	
		$B$	$\lambda_0$
W33	Parallel	1.1624	42.3371
	Normal	1.3326	53.7151
W37	Parallel	1.1386	53.1942
	Normal	1.6805	18.0213
W43	Parallel	1.1590	39.9623
	Normal	1.3131	37.4792

Table 8 Fitting size effect law of Eq. (3) by using trust-region nonlinear curve fitting

Mix ID	Placement and loading configuration	$f_{cu}(d) = \frac{Bf'_c}{\sqrt{1 + \frac{d}{\lambda_0 d_{max}}}}$			
		$B$	$\lambda_0$	$p$ -value for $B$	$p$ -value for $\lambda_0$
W33	Parallel	1.1820	31.876	$1.2611 \times 10^{-8}$	0.1469
	Normal	1.332	41.889	$1.7115 \times 10^{-8}$	0.2474
W37	Parallel	1.1488	45.384	$4.7810 \times 10^{-8}$	0.3253
	Normal	1.7497	11.276	$4.0807 \times 10^{-4}$	0.3491
W43	Parallel	1.1803	31.242	$5.7787 \times 10^{-8}$	0.2027
	Normal	1.4161	18.397	$8.3286 \times 10^{-5}$	0.3950

the statistical assessment of the fitting, the  $p$ -value of the coefficients, assuming a significance level of 5% were calculated, which are shown in Table 8.

As stated previously, if  $\lambda_0 \in [2,3]$  then the Eq. (3) could not be fitted. To illustrate this, for the test data of W33 mix in parallel configuration,  $\lambda_0$  assumed equal to 2.0. Then, the fitted line was drawn in Fig. 12. As it could be seen, the assumption could lead to wrong answers.

The other form of size effect, denoted as MSEL, is of the form of Eq. (4). The empirical coefficients of MSEL have been determined by using the trust-region algorithm

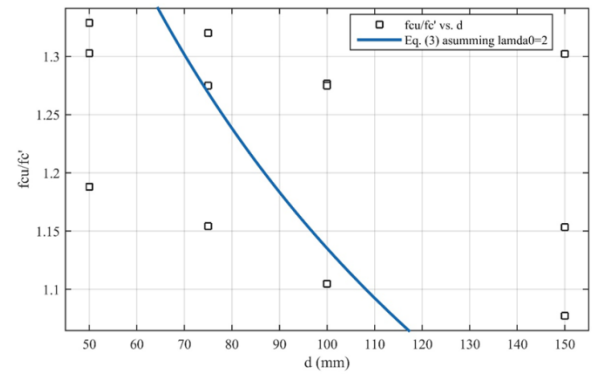


Fig. 12 The effect of presuming  $\lambda_0 \in [2,3]$  in fitting the size effect law of Eq. (3)

Table 9 Fitting size effect law of Eq. (4) by using trust-region nonlinear curve fitting

Mix ID	Placement and loading configuration	$f_{cu}(d) = \frac{Bf_c'}{\sqrt{1 + \frac{d}{\lambda_0 d_{\max}}}} + \alpha f_c'$					
		$B$	$\lambda_0$	$\alpha$	$p$ -value for $B$	$p$ -value for $\lambda_0$	$p$ -value for $\alpha$
W33	Parallel	2.1612	68.679	-0.9875	0.9636	0.9692	0.9834
	Normal	0.9421	25.83	0.3966	0.9314	0.9546	0.9718
W37	Parallel	0.4470	8.9229	7.3201	0.8354	0.9440	0.8354
	Normal*	124423	169270	-12421	0.1197	$2.5417 \times 10^{-18}$	0.1197
W43	Parallel	0.5403	5.6555	0.7014	0.5915	0.9205	0.6659
	Normal	0.9636	7.4650	0.5091	0.7922	0.9415	0.9156

\*The numerical solution of trust-region algorithm was ill condition for this case. Therefore, these model parameters may not be estimated well.

and have been tabulated in Table 9. As it can be observed in the normal configuration of mix W37, the numerical solution of trust-region algorithm of curve fitting was ill condition. However, the method converged successfully for other cases. Indeed, the convergence problem in highly nonlinear cases of numerical analysis could occur (Roudak *et al.* 2017, Roudak *et al.* 2017, Roudak *et al.* 2018, Roudak and Karamloo 2019).

In the case of curve fitting by the general form of Eq. (3), it was shown that the assumption of  $\lambda_0 \in [2,3]$  could lead to wrong answers. This condition, however, could be imposed in Eq. (4). This ranging for  $\lambda_0$  stems from the fact that in fracture mechanics of quasi-brittle materials, it is assumed that the area of fracture process zone is in proportion with maximum grain size. However, for the form of Eq. (3), the proposed range was not eligible for SCLC. In Table 10, by assuming  $\lambda_0 \in [2,3]$ , the trust-region algorithm was used and the empirical coefficients were re-estimated.

Comparing Table 10 and Table 9, one important question may raise. Which of the predictions are reliable for MSEL? Let us answer this question by fitting the calculated laws on the data corresponding to the mix W33 in parallel condition. To illustrate the situation, the results are shown in Fig. 13. As it could be observed, the empirical coefficients of Table 8 for Bazant's size effect law and Table 10 for MSEL are both correct. Nevertheless, fitting the form of Eq. (4) in an unconstraint condition could lead to unrealistic



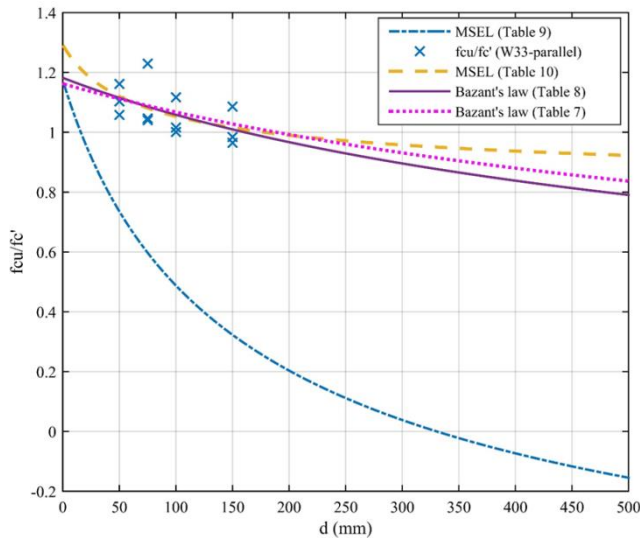


Fig. 13 Comparing the results of Table 7 to Table 10 with the test results of W33 mix in parallel configuration

answers. The other point, which could be deduced from Fig. 13, is that the Bazant's law could fit the results either by trust-region regression or by the proposed transformed coordinate system. However, authors believe that understanding the asymptotic condition of size effect laws needs more comprehensive wide-range tests and sophisticated facilities.

## 5. Conclusions

In the present paper, 81 specimens of different sizes were cast for three different self-compacting lightweight concrete mixes. All specimens were cured for 28 days under water at  $20 \pm 20^\circ\text{C}$ . By using the regression analysis, some empirical equations were obtained, which makes it possible to consider the effects of size and direction of loading for preliminary design purposes. Eventually, the following conclusions could be drawn:

- 1-Generally, the self-compacting lightweight concrete cubic samples had higher compressive strength than cylindrical samples. This trend is similar to normal concrete and self-compacting normal weight concrete.
- 2-The discrepancy between the strength of cubic specimens with those of cylinders decreases by increasing the sizes of cubes from 50 mm to 150 mm.
- 3- The ratios of cylindrical to cubic strength in parallel configuration were higher than those ratios for normal configuration.
- 4-The failure mechanism of self-compacting lightweight concrete specimens was similar to normal concrete. However, the size of specimens did not show a prominent effect on obliqueness of fracture.
- 5-Unconstraint trust-region curve fitting of modified size effect law could lead to erroneous results. However, the conventional size effect law should not be fitted with constraints.

Table 10: Fitting size effect law of Eq. (4) by using trust-region nonlinear curve fitting and assuming  $\lambda_0 \in [2,3]$

Mix ID	Placement and loading configuration	$f_{cu}(d) = \frac{Bf_c'}{\sqrt{1 + \frac{d}{\lambda_0 d_{max}}}} + \alpha f_c'$		
		B	$\lambda_0 \in [2,3]$	$\alpha$
W33	Parallel	0.5036	3	0.7886
	Normal	0.4667	3	0.9715
W37	Parallel	0.3813	2.949	0.8568
	Normal	1.366	3	0.6162
W43	Parallel	0.5175	2.992	0.7776
	Normal	0.8663	3	0.7226

## Acknowledgments

The authors would like to acknowledge the supports by Shahid Rajaee Teacher Training University

## References

- Akçay, B. and Tasdemir, M.A. (2009), "Optimisation of using lightweight aggregates in mitigating autogenous deformation of concrete", *Constr. Build. Mater.*, **23**(1), 353-363. <https://doi.org/10.1016/j.conbuildmat.2007.11.015>.
- Bazant, Z. and Pfeiffer, P. (1987), "Determination of fracture energy from size effect and brittleness number", *ACI Mater. J.*, **84**(6), 463-480.
- Bazant, Z.P. (1976), "Instability, ductility, and size effect in strain-softening concrete", *J. Eng. Mech.*, **102**(EM2), 331-344.
- Bazant, Z.P. (1982), *Crack Band Model for Fracture of Geomaterials*, Edmonton, Alberta.
- Bazant, Z.P. (1984), "Size effect in blunt fracture: concrete, rock, metal", *J. Eng. Mech.*, **110**(4), 518-535. [https://doi.org/10.1061/\(ASCE\)0733-9399\(1984\)110:4\(518\)](https://doi.org/10.1061/(ASCE)0733-9399(1984)110:4(518)).
- Bazant, Z.P. (1993), *Size Effect in Tensile and Compressive Quasibrittle Failure*.
- Bazant, Z.P. and Cedolin, L. (1979), "Blunt crack band propagation in finite element analysis", *J. Eng. Mech.*, **105**, 297-315.
- Bazant, Z.P., Kim, J.K. and Pfeiffer, P.A. (1986), "Nonlinear fracture properties from size effect tests", *J. Struct. Eng.*, **112**, 289-307.
- Bazant, Z.P. and Oh, B.H. (1983), "Crack band theory for fracture of concrete", *Mater. Struct.*, **16**, 155-177. <https://doi.org/10.1007/BF02486267>.
- Bazant, Z.P. and Xiang, Y. (1997), "Size effect in compression fracture: Splitting crack band propagation", *J. Eng. Mech.*, **123**(2), 162-172. [https://doi.org/10.1061/\(ASCE\)0733-9399\(1997\)123:2\(162\)](https://doi.org/10.1061/(ASCE)0733-9399(1997)123:2(162)).
- Bentz, D.P. (2009), "Influence of internal curing using lightweight aggregates on interfacial transition zone percolation and chloride ingress in mortars", *Cement Concrete Compos.*, **31**(5), 285-289. <https://doi.org/10.1016/j.cemconcomp.2009.03.001>.
- Bentz, D.P. and Snyder, K.A. (1999), "Protected paste volume in concrete: Extension to internal curing using saturated lightweight fine aggregate", *Cement Concrete Res.*, **29**(11), 1863-1867. [https://doi.org/10.1016/S0008-8846\(99\)00178-7](https://doi.org/10.1016/S0008-8846(99)00178-7).
- Blanks, R. and McNamara, C. (1935), "Mass concrete tests in large cylinders", *J. Proc.*, **31**(1), 280-303.
- BS EN 12390, p. (2000), Testing Hardened Concrete, Method of Determination of Compressive Strength of Concrete Cubes,

- British Standards Institution
- de Sensale, G.R. and Goncalves, A.F. (2014), "Effects of fine LWA and SAP as internal water curing agents", *Int. J. Concrete Struct. Mater.*, **8**(3), 229-238. <https://doi.org/10.1007/s40069-014-0076-1>.
- Di Bella, C., Villani, C., Hausheer, E. and Weiss, J. (2012), "Chloride transport measurements for a plain and internally cured concrete mixture", *ACI Mater. J.*, **290**, 1-16.
- EFNARC (2002), "Specification & guidelines for self-compacting concrete", English Edition, European Federation for Specialist Construction Chemicals and Concrete Systems, Norfolk, UK.
- Gonnermann, H.F. (1925), "Effect of size and shape of test specimen on compressive strength of concrete", *Proc. ASTM*, **25**, 237-250.
- Gyengo, T. (1938), "Effect of type of test specimen and gradation of aggregate on compressive strength of concrete", *J. Proc.*, **34**(1), 269-284.
- Hillerborg, A., Modeer, M. and Petersson, P.E. (1976), "Analysis of crack formation and crack growth in concrete by means of fracture mechanics and finite elements", *Cement Concrete Res.*, **6**, 773-782. [https://doi.org/10.1016/0008-8846\(76\)90007-7](https://doi.org/10.1016/0008-8846(76)90007-7).
- Hilsdorf, H.K. and Brammhuber, W. (1985), *Size Effects in the Experimental Determination of Fracture Mechanics Parameters*, Springer Netherlands, Dordrecht.
- Hubertova, M. and Hela, R. (2007), *The Effect of Metakaolin and Silica Fume on the Properties of Lightweight Self-Consolidating Concrete*, American Concrete Institute, Warsaw.
- Ince, R. and Çetin, S.Y. (2018), "Effect of grading type of aggregate on fracture parameters of concrete", *Mag. Concrete Res.*, 1-26. <https://doi.org/10.1680/jmacr.18.00095>.
- Kohno, K., Okamoto, T., Isikawa, Y., Sibata, T. and Mori, H. (1999), "Effects of artificial lightweight aggregate on autogenous shrinkage of concrete", *Cement Concrete Res.*, **29**, 611-614. [https://doi.org/10.1016/S0008-8846\(98\)00202-6](https://doi.org/10.1016/S0008-8846(98)00202-6).
- Karamloo, M. and Mazloom, M. (2018), "An efficient algorithm for scaling problem of notched beam specimens with various notch to depth ratios", *Comput. Concrete*, **22**(1), 39-51. <https://doi.org/10.12989/cac.2018.22.1.039>.
- Karamloo, M., Mazloom, M. and Payganeh, G. (2016), "Effects of maximum aggregate size on fracture behaviors of self-compacting lightweight concrete", *Constr. Build. Mater.*, **123**, 508-515. <https://doi.org/10.1016/j.conbuildmat.2016.07.061>.
- Karamloo, M., Mazloom, M. and Payganeh, G. (2016), "Influences of water to cement ratio on brittleness and fracture parameters of self-compacting lightweight concrete", *Eng. Fract. Mech.*, **168**, 227-241. <https://doi.org/10.1016/j.engfracmech.2016.09.011>.
- Karamloo, M., Mazloom, M. and Payganeh, G. (2017), "Effect of size on nominal strength of self-compacting lightweight concrete and self-compacting normal weight concrete: A stress-based approach", *Mater. Today Commun.*, **13**, 36-45. <https://doi.org/10.1016/j.mtcomm.2017.08.002>.
- Kim, H.K., Ha, K.A. and Lee, H.K. (2016), "Internal-curing efficiency of cold-bonded coal bottom ash aggregate for high-strength mortar", *Constr. Build. Mater.*, **126**, 1-8. <https://doi.org/10.1016/j.conbuildmat.2016.08.125>.
- Kim, H.K., Jeon, J.H. and Lee, H.K. (2012), "Workability, and mechanical, acoustic and thermal properties of lightweight aggregate concrete with a high volume of entrained air", *Constr. Build. Mater.*, **29**, 193-200. <https://doi.org/10.1016/j.conbuildmat.2011.08.067>.
- Kim, J.K. and Eo, S.H. (1990), "Size effect in concrete specimens with dissimilar initial cracks", *Mag. Concrete Res.*, **42**(153), 233-238. <https://doi.org/10.1680/mac.1990.42.153.233>.
- Kim, J.K., Yi, S.T., Park, C.K. and Eo, S.H. (1999), "Size effect on compressive strength of plain and spirally reinforced concrete cylinders", *ACI Struct. J.*, **96**(1), 88-94.
- Kong, L., Hou, L. and Du, Y. (2014), "Chemical reactivity of lightweight aggregate in cement paste", *Constr. Build. Mater.*, **64**, 22-27. <https://doi.org/10.1016/j.conbuildmat.2014.04.024>.
- Kumar, S. and Barai, S.V. (2012), "Size-effect of fracture parameters for crack propagation in concrete: a comparative study", *Comput. Concrete*, **9**(1), 1-19. <https://doi.org/10.12989/cac.2012.9.1.001>.
- L'Hermite, R. (1955), *Idées Actuelles sur la Technologie du Béton*, Documentation Technique du Bâtiment et des Travaux Publics, Paris.
- Leicester, R. (1969), "The size effect of notches.", *Proceedings of the Second Australasian Conference on Mechanics of Materials and Structures*, Melbourne.
- Lotfy, A., Hossain, K.M.A. and Lachemi, M. (2016), "Durability properties of lightweight self-consolidating concrete developed with three types of aggregates", *Constr. Build. Mater.*, **106**, 43-54. <https://doi.org/10.1016/j.conbuildmat.2015.12.118>.
- Mazloom, M., Allahabadi, A. and Karamloo, M. (2017), "Effect of silica fume and polyepoxide-based polymer on electrical resistivity, mechanical properties, and ultrasonic response of SCLC", *Adv. Concrete Constr.*, **5**(6), 587-611. <https://doi.org/10.12989/acc.2017.5.6.587>.
- Mazloom, M. and Karamloo, M. (2019), *Critical Crack-Tip Opening Displacement of SCLC*, Singapore.
- Mazloom, M. and Mahboubi, F. (2017), "Evaluating the settlement of lightweight coarse aggregate in self-compacting lightweight concrete", *Comput. Concrete*, **19**(2), 203-210. <https://doi.org/10.12989/cac.2017.19.2.203>.
- Mazloom, M., Saffari, A. and Mehrvand, M. (2015), "Compressive, shear and torsional strength of beams made of self-compacting concrete", *Comput. Concrete*, **15**(6), 935-950. <https://doi.org/10.12989/cac.2015.15.6.935>.
- Mazloom, M., Soltani, A., Karamloo, M., Hassanloo, A. and Ranjbar, A. (2018), "Effects of silica fume, superplasticizer dosage and type of superplasticizer on the properties of normal and self-compacting concrete", *Adv. Mater. Res.*, **7**(1), 45-72. <https://doi.org/10.12989/amr.2018.7.1.407>.
- Mazloom, M. and Yoosefi, M.M. (2013), "Predicting the indirect tensile strength of self-compacting concrete using artificial neural networks", *Comput. Concrete*, **12**(3), 285-301. <https://doi.org/10.12989/cac.2013.12.3.285>.
- Mindess, S. (1984), "The effect of specimen size on the fracture energy of concrete", *Cement Concrete Res.*, **14**(3), 431-436. [https://doi.org/10.1016/0008-8846\(84\)90062-0](https://doi.org/10.1016/0008-8846(84)90062-0).
- Moré, J.J. (1978), *The Levenberg-Marquardt Algorithm: Implementation and Theory*, Springer Berlin Heidelberg
- Neville, A.M. (1966), "A general relation for strengths of concrete specimens of different shapes and sizes", *J. Proc.*, **63**(10), 1095-1110.
- Nikbin, I.M., Beygi, M.H.A., Kazemi, M.T., Vaseghi Amiri, J., Rabbanifar, S., Rahmani, E. and Rahimi, S. (2014), "A comprehensive investigation into the effect of water to cement ratio and powder content on mechanical properties of self-compacting concrete", *Constr. Build. Mater.*, **57**, 69-80. <https://doi.org/10.1016/j.conbuildmat.2014.01.098>.
- Nikbin, I.M., Dehestani, M., Beygi, M.H.A. and Rezvani, M. (2014), "Effects of cube size and placement direction on compressive strength of self-consolidating concrete", *Constr. Build. Mater.*, **59**, 144-150. <https://doi.org/10.1016/j.conbuildmat.2014.02.008>.
- Roudak, M.A. and Karamloo, M. (2019), "Establishment of non-negative constraint method as a robust and efficient first-order reliability method", *Appl. Math. Model.*, **68**, 281-305. <https://doi.org/10.1016/j.apm.2018.11.021>.
- Roudak, M.A., Shayanfar, M.A., Barkhordari, M.A. and Karamloo, M. (2017), "A new three-phase algorithm for computation of reliability index and its application in structural

- mechanics", *MeReC*, **85**, 53-60.  
<https://doi.org/10.1016/j.mechrescom.2017.08.008>.
- Roudak, M.A., Shayanfar, M.A., Barkhordari, M.A. and Karamloo, M. (2017), "A robust approximation method for nonlinear cases of structural reliability analysis", *Int. J. Mech. Sci.*, **133**, 11-20. <https://doi.org/10.1016/j.ijmecsci.2017.08.038>.
- Roudak, M.A., Shayanfar, M.A. and Karamloo, M. (2018), "Improvement in first-order reliability method using an adaptive chaos control factor", *Struct.*, **16**, 150-156. <https://doi.org/10.1016/j.istruc.2018.09.010>.
- Sim, J.I., Yang, K.H., Kim, H.Y. and Choi, B.J. (2013), "Size and shape effects on compressive strength of lightweight concrete", *Constr. Build. Mater.*, **38**, 854-864. <https://doi.org/10.1016/j.conbuildmat.2012.09.073>.
- Tokay, M. and Özdemir, M. (1997), "Specimen shape and size effect on the compressive strength of higher strength concrete", *Cement Concrete Res.*, **27**(8), 1281-1289. [https://doi.org/10.1016/S0008-8846\(97\)00104-X](https://doi.org/10.1016/S0008-8846(97)00104-X).
- Topçu, İ.B. and Uygunoğlu, T. (2010), "Effect of aggregate type on properties of hardened self-consolidating lightweight concrete (SCLC)", *Constr. Build. Mater.*, **24**(7), 1286-1295. <https://doi.org/10.1016/j.conbuildmat.2009.12.007>.
- Vakhshouri, B. and Nejadi, S. (2017), "Compressive strength and mixture proportions of self-compacting lightweight concrete", *Comput. Concrete*, **19**(5), 555-566. : <https://doi.org/10.12989/cac.2017.19.5.555>.
- Walsh, P.F. (1972), "Fracture of plain concrete", *Ind. Concrete J.*, **46**(11), 469-470.
- Yazıcı, Ş. and İnan Sezer, G. (2007), "The effect of cylindrical specimen size on the compressive strength of concrete", *Build. Environ.*, **42**(6), 2417-2420. <https://doi.org/10.1016/j.buildenv.2006.06.014>.
- Yi, S.T., Yang, E.I. and Choi, J.C. (2006), "Effect of specimen sizes, specimen shapes, and placement directions on compressive strength of concrete", *NuEnD*, **236**(2), 115-127. <https://doi.org/10.1016/j.nucengdes.2005.08.004>.
- Zarghami, E., Azemati, H., Fatourehchi, D. and Karamloo, M. (2018), "Customizing well-known sustainability assessment tools for Iranian residential buildings using Fuzzy Analytic Hierarchy Process", *Build. Environ.*, **128**, 107-128. <https://doi.org/10.1016/j.buildenv.2017.11.032>.
- Zarghami, E., Fatourehchi, D. and Karamloo, M. (2017), "Impact of daylighting design strategies on social sustainability through the built environment", *Sustain. Develop.*, **25**(6), 504-527. <https://doi.org/10.1002/sd.1675>.
- Zhang, H., Šavija, B., Xu, Y. and Schlangen, E. (2018), "Size effect on splitting strength of hardened cement paste: Experimental and numerical study", *Cement Concrete Compos.*, **94**, 264-276. <https://doi.org/10.1016/j.cemconcomp.2018.09.018>.
- Zhao, Y.H., Chang, J.M. and Gao, H.B. (2015), "On geometry dependent R-curve from size effect law for concrete-like quasibrittle materials", *Comput. Concrete*, **15**(4), 673-686. <https://doi.org/10.12989/cac.2015.15.4.673>.
- Zhutovsky, S. and Kovler, K. (2012), "Effect of internal curing on durability-related properties of high performance concrete", *Cement Concrete Res.*, **42**(1), 20-26. <https://doi.org/10.1016/j.cemconres.2011.07.012>.
- Zhutovsky, S., Kovler, K. and Bentur, A. (2002), "Efficiency of lightweight aggregates for internal curing of high strength concrete to eliminate autogenous shrinkage", *Mater. Struct.*, **35**(2), 97-101. <https://doi.org/10.1007/BF02482108>.